This is a repository copy of *Multiplexed experimental strategies for fragment library screening against challenging drug targets using SPR biosensors*.

White Rose Research Online URL for this paper:
https://eprints.whiterose.ac.uk/id/eprint/204160/

Version: Published Version

Article:

FitzGerald, Edward A., Vagrys, Darius, Opassi, Giulia et al. (13 more authors) (2023) Multiplexed experimental strategies for fragment library screening against challenging drug targets using SPR biosensors. SLAS Discovery. ISSN: 2472-5552

https://doi.org/10.1016/j.slasd.2023.09.001

Multiplexed experimental strategies for fragment library screening against challenging drug targets using SPR biosensors

Edward A. FitzGerald [a,b], Darius Vagrys [c,d], Giulia Opassi [a], Hanna F. Klein [e], David J. Hamilton [f], Vladimir O. Talibov [a], Mia Abramsson [a], Anna Moberg [g], Maria T. Lindgren [g], Claes Holmgren [g], Ben Davis [c], Peter O'Brien [e], Maikel Wijtmans [f], Roderick E. Hubbard [c,d], Iwan J.P. de Esch [f], U.Helena Danielson [a,h],*

[a] *Department of Chemistry - BMC, Uppsala University, Uppsala, Sweden*
[b] *Beactica Therapeutics AB, Virdings allé 2, Uppsala, Sweden*
[c] *Vernalis (R&D) Ltd., Granta Park, Great Abington, Cambridge, United Kingdom*
[d] *YSBL, Department of Chemistry, University of York, York, United Kingdom*
[e] *Department of Chemistry, University of York, York, United Kingdom*
[f] *Amsterdam Institute of Molecular and Life Sciences (AIMMS), Division of Medicinal Chemistry, Faculty of Sciences, Vrije Universiteit Amsterdam, De Boelelaan 1108, 1081 HZ, Amsterdam, The Netherlands*
[g] *Cytiva, Björkgatan 30, Uppsala, Sweden*
[h] *Science for Life Laboratory, Uppsala University, Uppsala, Sweden*

ARTICLE INFO

ABSTRACT

Surface plasmon resonance (SPR) biosensor methods are ideally suited for fragment-based lead discovery. However, generally applicable experimental procedures and detailed protocols are lacking, especially for structurally or physico-chemically challenging targets or when tool compounds are not available. Success depends on accounting for the features of both the target and the chemical library, purposely designing screening experiments for identification and validation of hits with desired specificity and mode-of-action, and availability of orthogonal methods capable of confirming fragment hits. The range of targets and libraries amenable to an SPR biosensor-based approach for identifying hits is considerably expanded by adopting multiplexed strategies, using multiple complementary surfaces or experimental conditions. Here we illustrate principles and multiplexed approaches for using flow-based SPR biosensor systems for screening fragment libraries of different sizes (90 and 1056 compounds) against a selection of challenging targets. It shows strategies for the identification of fragments interacting with 1) large and structurally dynamic targets, represented by acetyl choline binding protein (AChBP), a Cys-loop receptor ligand gated ion channel homologue, 2) targets in multi protein complexes, represented by lysine demethylase 1 and a corepressor (LSD1/CoREST), 3) structurally variable or unstable targets, represented by farnesyl pyrophosphate synthase (FPPS), 4) targets containing intrinsically disordered regions, represented by protein tyrosine phosphatase 1B (PTP1B), and 5) aggregation-prone proteins, represented by an engineered form of human tau (tau K18^M). Practical considerations and procedures accounting for the characteristics of the proteins and libraries, and that increase robustness, sensitivity, throughput and versatility are highlighted. The study shows that the challenges for addressing these types of targets is not identification of potentially useful fragments per se, but establishing methods for their validation and evolution into leads.

1. Introduction

The first methods and concepts of fragment-based drug discovery (FBDD [1]) emerged over 25 years ago, and its subsequent adoption in academia and industry continues to increase. FBDD, in its essence, is a reductionist alternative to high-throughput screening (HTS), built on the theory that a much broader chemical space can be more efficiently probed by using structurally diverse compounds with lower molecular weight than one would conventionally find in a HTS or a drug-like compound library. Its core principles are accepted as viable means for
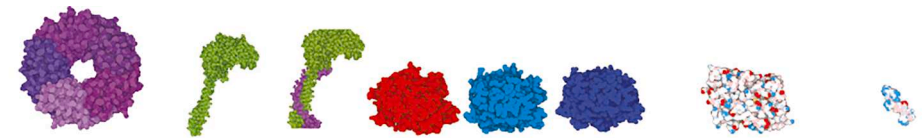
Table 1

Overview of target proteins, assay design, fragment libraries used and screening outcomes. Targets and their structural characteristics: acetylcholine binding protein (AChBP), lysine demethylase 1 (LSD1) with and without the protein cofactor CoREST, farnesyl pyrophosphate synthase (FPPS) from, *trypanosoma cruzi, brucei* and human (tc, tb and h, respectively), the catalytic domain of protein tyrosine phosphatase 1B (PTP1B) in two different lengths (1–301 and 1–393, respectively) and tau K18^{M}. SPR biosensor assay design with experimental details. Screening strategy and results from different steps.

		AChBP	LSD1	LSD1/COREST	hFPPS	tbFPPS	tcFPPS	PTP1B$_{1-301}$	PTP1B$_{1-393}$	Tau K18^{M}
Targets	Attributes	Large and Structurally Dynamic	Multi-Protein Complexes		Structurally Variable or Unstable			Containing Intrinsically Disordered Regions		Aggregation-Prone
	Molecular mass (kDa)	125	74.5	96.4	40.6	42.1	41.3	38	46	14.5
	Theoretical pI	4.85	7.22	5.87	5.12	4.88	5.33	6.1	6.16	9.73
Assay design	Immobilization	His capture, crosslinked	amine	amine	amine	amine	amine	amine	amine	amine, streptavidin
	Sensor chip	NTA	CM7, CM5	CM7,CM5	CM5	CM5	CM5	CM5	CM5	CM5, SA
	Immobilization level (RU)	~5000	~23000, ~6000	~26000, ~6000	~3000	~3000	~3000	~6000 to ~8000	~9000 to ~11000	~2000 to ~4000
	Expected R$_{max}$	35	35-45	35-45	20	20	20	26-32	20-31	23-31
	Assay buffer	PBS-T + 2 mM DTT	HBS-T + 1 mM DTT		HBS-T + 3 mM MgCl$_2$, 1 mM TCEP			TBS-T + 1 mM DTT		TBS-T + 1 mM DTT
	Ref compounds	lobeline	BEA1	not available	not available	not available	not available	suramin		not available
Screening	Fragment library	FL1056	FL1056	FL1056	FL90	FL90	FL90	FL1056		FL1056
	Screening conc. (μM)	250	250	250	250	250	250	500		500
	Excluded fragments	32	13	6	-	-	-	10	9	8
	Identified hits	107	107	110	13	11	14	107	107 + 22†*	107
	Confirmed hits	10	11	5	6	4	5	10	9 + 0	45 (19*)

* - prioritized fragments exhibiting large structural differences
† - selected fragments that exhibit higher binding to PTP1B(1-393) than PTP1B(1-301) in primary screen
• - confirmed fragments from BLS screen (†) to bind specifically to PTP1B(1-393)

finding and evolving hits for a chemical biology or drug discovery project [2]. Fragments are compounds that fulfil some basic structural features (MW < 300 Da, clogP < 3, hydrogen bond acceptors (HBA) ≤ 3, hydrogen bond donors (HBD) ≤ 3) although the criteria are not strict [3, 4].

FBDD has been a truly transformative approach, proven to be effective for the discovery of novel therapeutics and with various examples in the clinic, including six FDA-approved drugs to date: vemurafenib [5], erdafitinib [6], venetoclax [7], pexidartinib [8], asciminib [9], sotorasib [10]. Now that fragment libraries have become commercially available and screening technologies are cheaper to acquire and implement, FBDD is a realistic option for smaller pharmaceutical companies and contract research organizations, as well as for academic core facilities and research groups. Nevertheless, success relies heavily on the capability to use sophisticated biophysical instrumentation, as well as access to appropriate forms of the target protein and suitable fragment libraries.

Surface plasmon resonance (SPR)-based biosensors were amongst the earliest technologies adopted for FBDD [11]. Their sensitivity and throughput are suitable for fragment library screening and the flexible experimental design and information rich data output makes the technology useful also for supporting the evolution of hits and optimisation of leads all the way to nomination of candidate drugs [12]. Their use has increased over time and experimental strategies and applications are continuing to evolve [13]. In addition, new SPR-based biosensors developed specifically for FBDD have appeared on the market. They have increased sensitivity, throughput and methodological features allowing experiments to be purposefully designed and analysed for fragment-based research. Although the application of SPR biosensors for FBDD requires lower quantities of protein than other common methods used for FBDD, the protein must be stable and in a functional form after immobilisation to sensor surfaces and throughout the experimental procedure. However, detailed protocols or descriptions of generally suitable experimental procedures are lacking and disclosed methods for more challenging targets is limited. The experimental strategy must be defined on a case-by-case basis, driven by a good understanding of the target characteristics and the types of lead compounds and modes-of-action that are of interest.

Herein, we outline novel SPR biosensor-driven strategies for identifying fragment hits, the first step in a FBDD project. (For a basic background on using SPR biosensors for FBDD, see Supplemental Information (SI) 1.) We have here used two flow-based SPR biosensors with different technical features, two fragment libraries of different sizes and composition and a panel of five physico-chemically challenging target proteins (nine variants in total) representing different target classes, size, structural complexity and/or lacking tool compounds (Table 1).

Acetylcholine binding protein (AChBP) is a soluble homologue of human Cys-loop receptors, such as the nicotinic α7 receptor [14]. It lacks the trans-membrane domain present in this class of ligand-gated ion channels (LGICs) but encompasses the extracellular ligand-binding domain and the regulatory binding sites. Interestingly, binding of ligands to AChBP induces similar conformational changes as in the human receptors, with a conserved activation mechanism. Although SPR biosensor technology has been used for studies of LGIC interactions, it has so far only been demonstrated for recombinant homo pentamers [15]. AChBP and engineered variants are simpler options and have been found to be good starting points for the identification of novel ligand scaffolds interacting with binding sites in the ectodomain of LGICs [16]. For evolution of fragments into functional modulators, as agonists or antagonists, it is essential to use orthogonal assays that identify the binding site and effects of ligand binding on the structure for the actual target protein, or functional assays [16]. Still, the pentameric structure and large size (Mw = 125 kDa) of AChBP makes a biosensor-based fragment-based lead discovery (FBLD) challenging due to many potential binding sites, while the acidic isoelectric point (pI = 4.85) makes it difficult to immobilise the protein using the standard amine coupling procedure. Moreover, since ligand binding can induce conformational changes that distort sensorgrams, detection of hits is challenging [17].

Lysine demethylase 1 (LSD1) is an epigenetic target initially described in 2004 as the first histone tail demethylating enzyme [18]. LSD1 is a multidomain protein with a molecular weight of 74.5 kDa. It uses FAD as a catalytic cofactor and its function is regulated by several binding partners. The catalytic activity of LSD1 is dependant on CoREST,

a co-repressor protein that stabilizes its structure by binding to the tower domain. Other chromatin proteins and nucleosomes also interact with LSD1, further regulating its function [19]. LSD1 has a complex biology and various potential roles in cancer [20]. There is consequently an interest in compounds targeting both its catalytic function and interfering with its interactions with the cofactor CoREST as well as with other proteins [21]. A strategic question when screening a library against LSD1 is what form of the protein should be used (LSD1 alone or the LSD1/CoREST complex) and what sites on the protein are relevant for ligand binding (*e.g.* the catalytic site or a protein-protein interaction site).

Farnesyl pyrophosphate synthase (FPPS) is a Mg^{2+}-dependant regulatory enzyme with a key role in the isoprenoid biosynthetic pathway and a target for osteoporosis and cancer therapy (hFPPS), as well as for new drugs against trypanosomiasis (tbFPPS, tcFPPS) [22,23]. Although bisphosphonate substrate analogues are potential inhibitors for all FPPS isoforms, allosteric inhibitors have also been identified for the human isoform [24,25]. Allosteric ligands with novel scaffolds or binding sites are relevant for all three variants of FPPS and it has been reported that they have inhibitory effects in pancreatic cancer cells [26]. However, they have not yet been reported for tbFPPS or tcFPPS. The latter could result in antiparasitic drugs that do not target the human enzyme. However, the lack of tool compounds validating the functionality of the parasitic isoforms requires a creative experimental design, but that can provide information about hit selectivity.

Protein tyrosine phosphatase 1B (PTP1B) is a 434 aa protein with a folded N-terminal catalytic phosphatase domain (*ca.* 301 aa), a disordered proline-rich regulatory domain involved in protein-interactions (*ca.* 90 aa), and a hydrophobic C-terminal ER-targeting domain (*ca.* 40 aa) [27]. The protein is involved in diabetes, obesity development and mammary tumorigenesis. The identification of proteins with intrinsically disordered regions (IDRs) has changed our understanding of the link between protein structure and function, and the importance of such interactions for regulation in mammalian biology [28]. There is consequently great interest exploring the possibilities of targeting and modulating intrinsically disordered proteins (IDPs) with LMW ligands, with recent promising results [29]. The lack of tool compounds and elusive structure of PTP1B makes it a challenging target for a biophysics-based approach.

Human tau is an IDP involved in forming neurofibrillary tangles in Alzheimer's disease [30]. Tau K18 is a truncated form encompassing four paired helical filaments (PHFs) containing hexapeptide motifs at the core of formed fibrils. Fibril formation is enhanced by oxidation of Cys-residues, why mutation of C291 and C322 to serine (C291S, C322S) can be used to generate a stable protein in the form of a monomer [31, 32]. This protein also represents a very challenging target class for a biophysics-based approach, for similar reasons as PTP1B.

The results from this study show that these challenging targets are all amenable to an SPR biosensor-based screening approach. By adopting a multiplexed strategy, the performance of the screening of a fragment library was considerably improved. However, the validation and progression of hits into leads requires orthogonal approaches that are suited to the targets in question which was out of scope for the work presented here.

2. Materials and methods

2.1. Fragment libraries

Fragment library FL1056 is comprised of 1056 fragments collated from SciLifeLab [33] and FragNet compound collections selected on the basis of key physicochemical properties, including heavy atom count (HAC), molecular weight (MW) and calculated lipophilicity (cLogP). The selection criteria essentially matched the guidelines put forward by Astex for typical fragments (MW < 300 Da, clogP < 3, HBA ≤ 3, HBD ≤ 3) [3,4]. The FragNet collection includes 3D fragments, *i.e.* compounds

that are not flat, but with a more complex structure. FL90 (Frag Xtal Screen library, JENA Bioscience) comprises 90 fragments characterized by a large chemical diversity and high solubility and suited for crystallography [34].

The structural diversities of the two fragment libraries [35] were determined by first generating the 3-dimensional structures of the fragments using Pipeline Pilot 16.5.0.143, 2016, Accelrys Software Inc. Prior to conformer generation a wash step was performed, which involved stripping salts and ionising the molecule at pH 7.4. SMILES strings were converted to their canonical representation and the original stereochemistry at each chiral centre was recorded. Any stereo centre created during the ionisation would have undefined stereochemistry. A SMILES file was written that contained all possible stereoisomers of the molecule. Conformers were generated using Catalyst with the BEST conformational analysis method and relative stereochemistry. Catalyst was run directly on the server and not through the built-in Conformation Generator component. The maximum relative energy threshold was left at the default 20 kcal mol^{-1} and a maximum of 255 conformers were generated for each compound. The aim of this was to give the best possible coverage of conformational space. The resulting conformations from Catalyst were read and only those where the stereochemistry matched the original molecule or its enantiomer were kept. These were then all standardized to the original stereochemistry by mirroring the coordinates of the enantiomers. Duplicate conformations were filtered with a Root Mean Square Deviation (RMSD) threshold of 0.1. Each conformation was minimized using 200 steps of Conjugate Gradient minimization with an RMS gradient tolerance of 0.1. This was performed using the CHARMm forcefield with Momany-Rone partial charge estimation and a Generalized Born implicit solvent model. After minimization, duplicates were filtered again with a RMSD threshold of 0.1.

Generated conformations were used to generate the three Principal Moments of Inertia (PMI) (I1, I2 and I3) which were then normalized by dividing the two lower values by the largest (I1/I3 and I2/I3) using Pipeline Pilot built-in components. PMI about the principal axes of a molecule were calculated according to the following rules: 1. The moments of inertia are computed for a series of straight lines through the centre of mass. 2. Distances are established along each line proportional to the reciprocal of the square root of I on either side of the centre of mass. The locus of these distances forms an ellipsoidal surface. The principal moments are associated with the principal axes of the ellipsoid.

Cumulative PMI analysis was performed in the following way. First, the normalized principal moment of inertia ratio (NPR) was calculated for each conformer and the sum ΣNPR calculated as NPR1 + NPR2. The mean ΣNPR for each fragment was then obtained. This value was used as a measure of the three-dimensionality of each fragment. The cumulative percentage of fragments within a defined distance from the rod-disc axis (ΣNPR) was calculated and plotted.

MW, HAC, clogP, number of HBD and HBA, rotatable bond count (RBC), fraction of sp3 carbons (Fsp3) and topological polar surface area (TPSA) were calculated using RDKit v3.4 in KNIME v3.5.2. Prior to calculation, salts were stripped and canonical SMILES were generated. clogP values were calculated using Daylight/BioByte ClogP v4.3.

2.2. Surface plasmon resonance biosensor experiments

Biosensor experiments were performed using Biacore 8K+ or Biacore T200 instruments (Cytiva, Uppsala, Sweden). The Biacore T200 was used for an initial screen of FL90 against FPPS, and for validation of the FPPS hits identified in the Biacore 8K+ based screen.

2.3. Target proteins and biosensor surface preparations

Protein purities were estimated by SDS-PAGE and concentrations by NanoDrop ND-1000 Spectrophotometer (Marshall Scientific). Thermal stabilities of proteins in different buffers and the potential stabilizing effects of ligands were evaluated using a direct thermal shift assay using

a Tycho NT6 instrument (Nanotemper Technologies), monitoring intrinsic protein fluorescence at 330 and 350 nm during a thermal ramp from 35 °C to 95 °C. Data were plotted as a derivative to get the inflection point for the intrinsic fluorescence shift from which the inflection temperature (T_i) was determined. Samples were prepared by diluting protein and compound to a final concentration of 1 μM and 1 mM, respectively. The buffers used for immobilisation of the target proteins are summarised in Table SI 2_1.

2.3.1. Acetylcholine binding protein (AChBP)

His-tagged acetylcholine binding protein (AChBP) from *Lymnaea stagnalis* was used for these experiments. The protein was expressed and purified as previously described [36,37]. The surface of Sensor Chip NTA (Cytiva) was first conditioned with 1 min injection of regeneration solution 10 μL/min at 25 °C. This was followed by injection of running buffer to remove any excess regeneration solution. Next, the surface was prepared by injecting a 1 min pulse of 0.5 mM $NiCl_2$ at 5 μL/min, with a subsequent wash step with running buffer supplemented with 3 mM ethylenediaminetetraacetic acid (EDTA). The surface of the sensor chip was subsequently activated using 1:1 mixture of 400 mM 1-ethyl-3-(3--dimethylaminopropyl)carbodiimide (EDC) 100 mM N-hydroxysuccinimide (NHS) for 420 s at 10 μL/min at 25 °C. This was followed by injection of 10 μg/mL AChBP in the immobilization buffer for appropriate time at 10 μL/min until an immobilization level of ~4000 response units (RU), corresponding to a theoretical R_{max} of 20–40 RU for a 150 Da fragment. Eight start-up cycles were used for stabilizing the surface after the immobilization.

2.3.2. Lysine specific demethylase 1 (LSD1) & LSD1/corest

$LSD1_{172–833}$ and $LSD1_{172–833}$/$COREST_{308–485}$ were produced as previously described [38]. Both the LSD1 and the CoREST constructs consisted of a N-terminal hexahistidine tag followed by a thrombin cleavage site. Individually purified His-tagged LSD1 and His-tagged CoREST were combined and the binary complex isolated.

The surface of Sensor Chip CM5 or Sensor Chip CM7 (Cytiva) was activated using 1:1 mixture of 400 mM EDC/100 mM NHS for 420 s at 10 μL/min at 25 °C. This was followed by injection of 10 μg/mL $LSD1_{172–833}$ or $LSD1_{172–833}$ in a 1:1 complex with $CoREST_{308–485}$ in the immobilization buffer, for the appropriate time at 5 μL/min. The surface was then deactivated with Tris-buffered saline (TBS) with Tween (TBS-T) with three injections of 420 s at 10 μL/min. The reference flow cell was activated and deactivated using the same protocol, but without protein.

2.3.3. Farnesyl pyrophosphate synthase (FPPS)

Production of N-terminally His-tagged farnesyl pyrophosphate synthase from *Trypanosoma cruzi* (tcFPPS), *Trypanosoma brucei* (tbFPPS) and *human* (hFPPS) were carried out as previously described for tcFPPS [39]. Proteins were concentrated via centrifugation using a filter with a 30 kDa cut-off (Amicon Ultra-15), and the buffer was exchanged to storage buffer using PD10 columns (Cytiva). The storage buffer was 25 mM HEPES, 5 mM $MgCl_2$ and 1 mM TCEP pH 6.5, supplemented with 100 mM NaCl for hFPPS, 25 mM NaCl for tbFPPS and 200 mM NaCl for tcFPPS. Aliquots of the enzymes were flash-frozen in liquid nitrogen and stored at −80 °C.

The proteins were immobilized via amine coupling to Sensor Chip CM5 (Cytiva) at 25 °C and at a flow rate of 10 μL/min, using standard procedures [40]. For all three enzymes, the running buffer used for immobilization consisted of 10 mM (4-(2-hydroxyethyl)−1-piperazineethanesulfonic acid) (HEPES), 150 mM NaCl, 3 mM $MgCl_2$, 1 mM Tris carboxy ethyl phosphene (TCEP) and 0.05 % Tween-20. The surfaces were activated using a 1:1 mixture of 400 mM EDC and 100 mM NHS for 210 s. The protein was injected at 50 μg/mL and 5 μL/min for a time resulting in an immobilization level of ~3000 to 5000 RU, generating a theoretical R_{max} of ~20 RU for a fragment molecule of ~150 Da. Unreacted carboxyl groups remaining on the surface were deactivated with 1 M ethanolamine chloride (pH 8.5) for 210 s.

2.3.4. Protein tyrosine phosphatase 1B (PTP1B) $PTP1B_{1–301}$/ $PTP1B_{1–393}$

The catalytic domain (residues 1- 301) of human protein tyrosine phosphatase 1B with a N-terminal 6xHis tag ($PTP1B_{1–301}$) and the catalytic domain with the disordered region, with a N-terminal GST tag and a C-terminal 6xHis tag ($PTP1B_{1–393}$), were used for the experiments (see SI 2 for production protocols). The surface of a Sensor Chip CM5 (Cytiva) was activated using a 1:1 mixture of 400 mM EDC/100 mM NHS for 420 s at 10 μL/min at 25 °C. This was followed by injection of 25 μg/mL $PTP1B_{1–301}$ or $PTP1B_{1–393}$ in 10 mM sodium acetate pH 5.5, 1 mM dithiothreitol (DTT) at 10 μL/min to achieve R_{max} of approx. 20–40 RU for 150 Da fragments. The surface was then deactivated with 1 M ethanolamine for 420 s at 10 μL/min. The reference flow cell was activated and deactivated using the same protocol but without protein.

2.3.5. Tau K18^M

An engineered human tau construct (tau K18^M) corresponding to the paired helical filaments binding domain (residues 244–372), with C291S and C322S substitutions keeping it as a stable monomer and biotinylated and isotopically labelled constructs were produced as previously described [34].

Two different immobilisation methods were used. First, the surface of a Sensor Chip CM5 (Cytiva) was activated using 1:1 mixture of 400 mM EDC/100 mM NHS for 420 s at 10 μL/min at 25 °C. This was followed by injection of 25 μg/mL tau K18^M in 10 mM sodium borate pH 8.5 at 10 μL/min to achieve R_{max} values of approx. 20–40 RU for 150 Da fragments. The surface was then deactivated with 1 M ethanolamine for 420 s at 10 μL/min. The reference flow cell was activated and deactivated using the same protocol but without protein.

Second, the protein was biotinylated and captured to a streptavidin surface. The surface of Sensor Chip SA (Cytiva) was first conditioned with three consecutive 1 min injections of 1 M NaCl and 50 mM NaOH at 10 μL/min at 25 °C. This was followed by injection of 100 nM biotinylated protein in 50 mM HEPES pH 7.4, 150 mM NaCl, 0.05 % Tween-20 at 5 μL/min to achieve theoretical R_{max} value of 20–40 RU for a 150 Da fragment. Eight start-up cycles were used for stabilizing the surface after the immobilization. Running buffer of 25 mM Tris–HCl pH 7.4, 150 mM NaCl, 2 mM EDTA, 1 % DMSO was used for all fragment screening assays. Solvent correction was performed from 0.5 to 1.8 %.

2.4. Fragment library screening

2.4.1. Screening of fragment library FL1056

Fragment library FL1056 was screened against AChBP, LSD1, PTB1B and tau K18^M at 25 °C or 15 °C depending on target stability. The library was pre-screened at a high, single concentration, before use with a new target [41]. The procedure is also known as a "clean screen" [42]. The procedure involves injecting fragments at 500 μM over sensor surfaces prepared as for the actual screen and using the same experimental conditions, but a shorter cycle time (10 s contact time and 0 s dissociation). Fragments resulting in baseline changes between injections of at least 10 RU were excluded from subsequent screening experiments.

After removal of potentially problematic fragments from the library, the screening was done by injecting fragments with a 30 s contact time and 15 s dissociation time over target protein and appropriate reference surfaces at a single concentration in the running buffer suited for each target (Table 1). The flow system was washed with 50 % DMSO after each cycle. Reference compounds (Table 1) were injected each 36th cycle as a control for surface functionality over time. DMSO solvent correction and reference surfaces were set-up in the same manner as for the single channel system. Positive control for validation of surface functionality was lobeline for AChBP, and BEA1 (a gift from Beactica Therapeutics, Uppsala, Sweden) for LSD1 (see Fig. SI 2_1). When suitable tool compounds were lacking, theoretically calculated R_{max} values were used instead of experimental R_{max} values. In order to triage hits, a reductionist approach was taken and approximately the top 10 % of hits, *i.e.* with the highest response and without undesired kinetics (slow

association, slow dissociation or $R_{eq} >> R_{max}$, Fig. SI 1_3) were prioritized. FL1056 hits were confirmed in a two-fold dilution series starting at 250 or 500 μM, depending on the target (see Table 1) for 30 s at a flow rate of 30 μL/min., using a multi-channel system. Zero concentration injections were used for blank subtraction.

A comparative screening of FL1056 was carried out against PTP1B$_{1-301}$ and PTP1B$_{1-393}$. Suramin was injected at 7.5 μM as a positive control in the screen. Experiments were performed in 25 mM Tris–HCl pH 7.4, 150 mM NaCl, 2 mM EDTA, 1 mM DTT, 1 % dimethyl sulfoxide (DMSO). Solvent correction was done with 0.5 to 1.8 % DMSO. A hit threshold was set to 1 RU, based on blank controls, and 50 % of normalized signals were used to distinguish hits specific for IDRs.
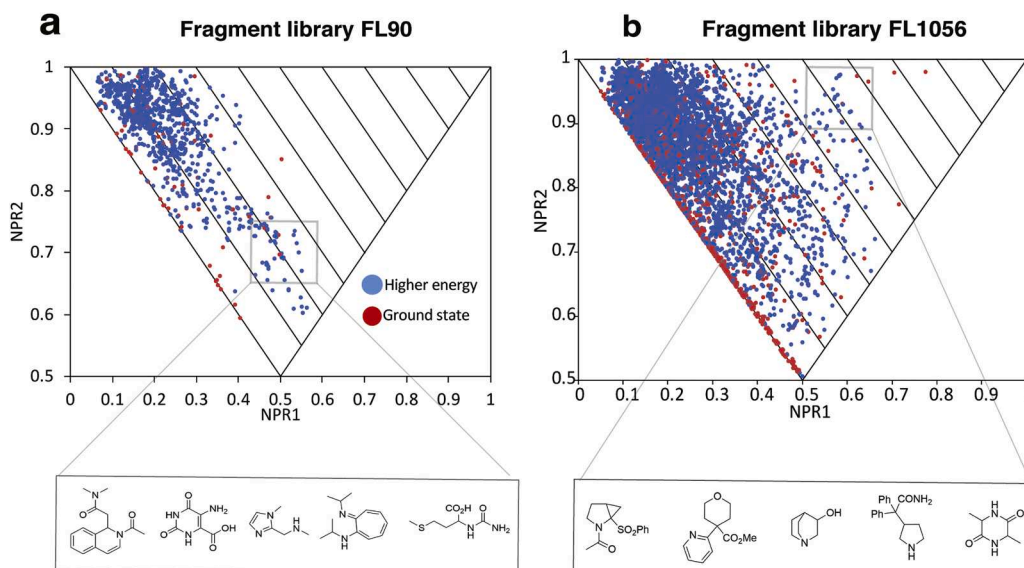
2.4.2. Screening of fragment library FL90

Fragment library FL90 was screened against hFPPS, tcFPPS and tbFPPS at 25 °C using a Biacore T200 instrument in the first screen, later repeated using Biacore 8K+ system (Cytiva). Pre-screening was not performed on FL90 since suitable screening conditions had already been identified for FPPS and FL90 [39]. For all three enzymes, the running buffer used for screening and interaction analysis consisted of 10 mM HEPES, 150 mM NaCl, 1 mM TCEP and 0.05 % Tween20, supplemented with 1 % DMSO. Screening was carried out in the presence and absence of 3 mM MgCl$_2$ in the buffer to discriminate binding to functional and non-functional targets.

Fragments were injected for 60 s at a flow rate of 50 μL/min in a final concentration of 250 μM. Fragments with signals between 30 % and 100 % of a theoretical R_{max} were selected as hits. The analysis was based on the average report point signal 6 s after the beginning of the injection (binding early response) in order to compensate for secondary effects. Binding early values were normalized (R_{norm}) with respect to the theoretical R_{max} of each fragment (as in Eq. (1)), in order to account for differences in molecular weight and protein immobilization levels.

$$R_{norm} = \left(RU_{analyte} \cdot \frac{MW_{protein}}{MW_{analyte} \cdot R_{protein}} \right) \tag{1}$$

where $RU_{analyte}$ is the signal for the analyte (injected fragment), $MW_{protein}$ and $MW_{analyte}$, the molecular weights for the protein and analytes, respectively and $R_{protein}$ is the immobilization level of the protein. The selected hits were validated on Biacore T200 (Cytiva) by analysis of the fragments in a 3-fold dilution series starting at 250 μM for 60 s at a flow rate of 50 μL/min.

2.4.3. Data analysis

Non-specific signals were removed by subtraction of reference surface signals from the target protein surface signals, and solvent corrections were performed with 8-point samples at appropriate DMSO concentrations to compensate for differences in DMSO concentrations. Apparent K_D values were estimated by steady state analysis by fitting dose response curves and a 1:1 binding model with free R_{max} (SI 1, Equation 2).

Hits from concentration series experiments that show little curvature (far from saturation) were ranked on the basis of K_D or Binding Efficiency (BE) values, calculated as the initial slope of the linear relationship between complex concentration (in R_{norm}) and ligand concentrations at very low ligand concentrations [43]. The hit threshold was set to 30 % of the theoretical R_{max} of each compound, with a limit at 100 %. The data from all screens were evaluated with Biacore Insight Evaluation Software (Cytiva).
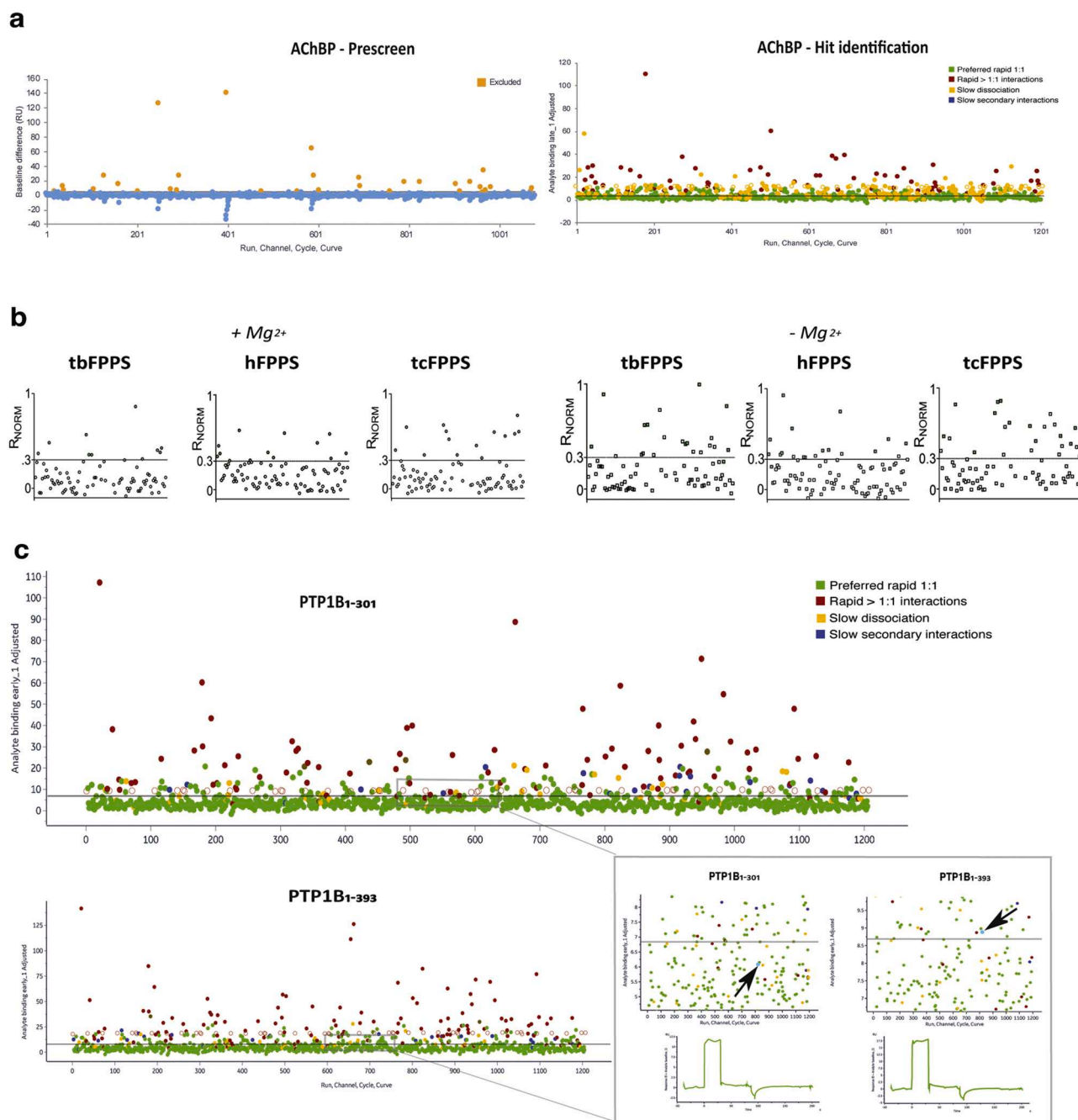
3. Results

3.1. Selection and characterization of fragment libraries

Strategies suitable for screening of fragment libraries depend primarily on library size. Here we illustrate screening using two different libraries. FL1056 is a unique library with compounds collated from several sources, including specifically designed 3D fragments. FL90 is a commercially available, simple and cost-efficient alternative. A principal moments of inertia (PMI) analysis (Fig. 1) shows that FL90 (Fig. 1a) has a significantly lower spatial complexity than FL1056 (Fig. 1b), consistent with the inclusion of novel 3D fragments in FL1056.

3.2. Library pre-screening and screening routines

The FL1056 was pre-screened before use to remove compounds that potentially interfere with the analysis of subsequently injected compounds. The advantage is illustrated with a representative dataset for FL1056 and AChBP (Fig. 2a). Troublesome fragments that give rise to large signals or that stick non-specifically to the surface were identified by distorted signals with a high response and trailing signals in subsequent injections. The signal levels for fragments in the pre-screen is shown in Fig. 2a, left and for the screen in Fig. 2a, right. It can be seen that some troublesome fragments blocked the surface, resulting in a negative base line shifts in Fig. 2a, left, a phenomenon not seen in Fig. 2a, right. The pre-screening routine resulted in omitting

Fig. 1. Analysis of structural diversity of fragment libraries. Principal moments of inertia (PMI) analysis for all conformations up to 1.5 kcal mol^{-1} above the energy of the ground state conformation for each fragment. Triangular PMI plots show fragments with disc shapes at the bottom, rod shapes at the top-left and spherical shapes at the top-right. Conformations that lie furthest from the diagonal rod-disc axis have the most complex 3D shape as they deviate the most from planarity. a, FL90 and b, FL1056. Red dots indicate ground state conformers and blue dots show higher energy conformers. .

Fig. 2. Data illustrating typical outcomes from three stages of fragment library screening. a. Screen of FL1056 against AChBP. Left: Signals from pre-screen and identified fragments for exclusion (pink dots). Right: Screen of library with problematic fragments removed. The colour coding is based on fragment kinetic profiles (SI 1, Fig. 3): preferred rapid 1:1 without or with secondary effects after ligand binding (light and dark green, respectively), super stoichiometric rapid interactions >1:1 (red), slow dissociation (yellow) and slow secondary interactions in the association phase (blue). b. Screen of FL90 against FPPS from *human, trypanosoma cruzi* and *brucei* in the presence (left) and absence (right) of the cofactor Mg^{2+}. Fragments with normalised signals (R_{norm}) between 0.3 and 1 in the presence of Mg^{2+} were defined as hits (green). c, Screen of FL1056 against $PTP1B_{1-301}$ (top) and $PTP1B_{1-393}$ (bottom). A black arrow marks a fragment identified as a hit for one target but not the other (inset).

approximately 1 % of the compounds, depending on the experiment/target, *i.e.* on the experimental conditions used in each case (Table 1). However, since the contact time in the pre-screen is much shorter than in the binding level screen, it does not detect all problematic compounds.

To avoid super-stoichiometric binding and solubility problems, it is recommended to screen libraries at as low concentration as possible while still getting reliable signals. The Ligand Efficiency (LE) that can be expected for hits can be estimated on the basis of K_D values and HAC. For FL1056, the LEs of potential hits is shown in Table SI 1_1. When
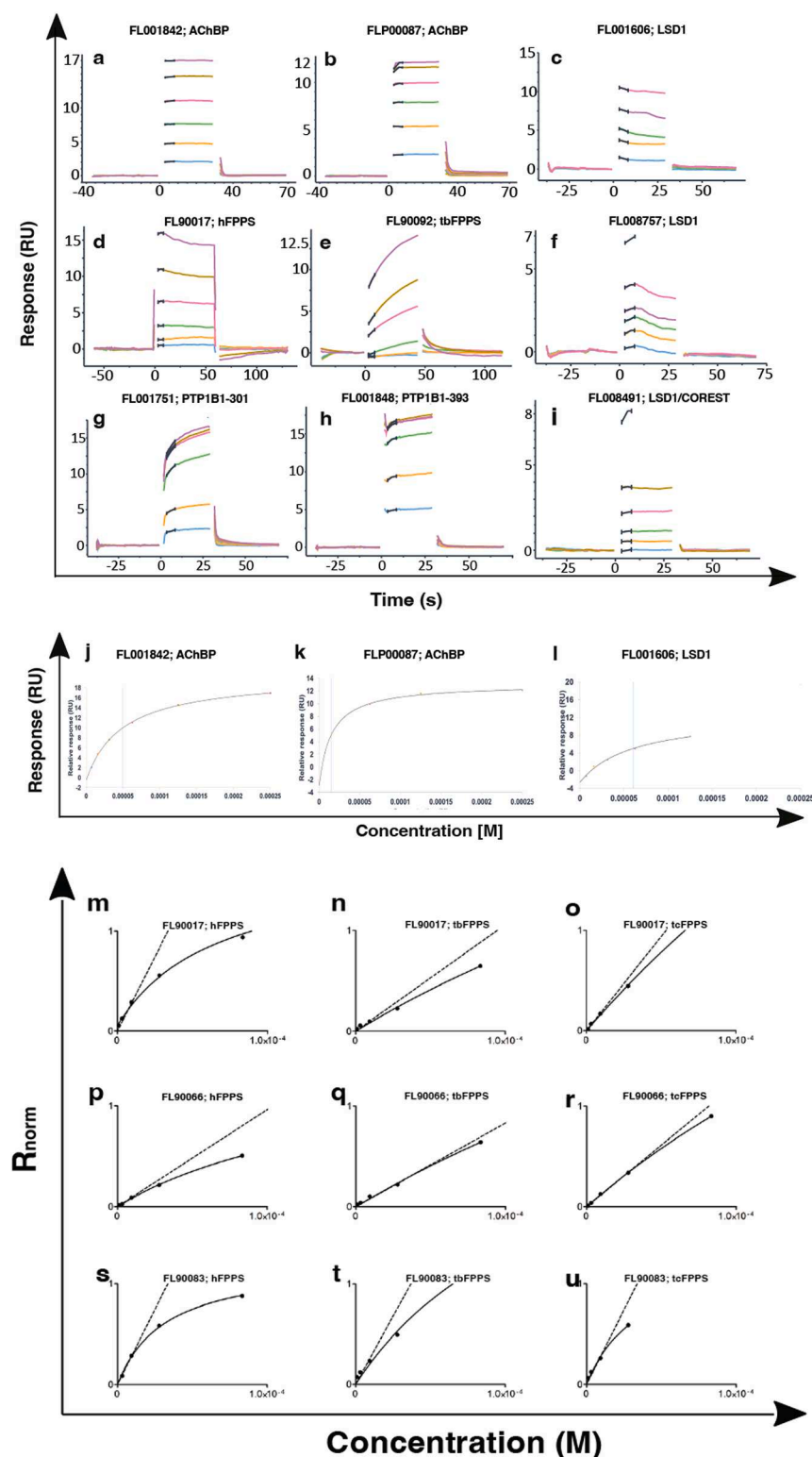
screening the library at 250–500 μM (suitable from the perspective of compound solubility), only fragments with $K_D < 1$ mM can be expected to result in > 50 % fractional occupancy (Fig. SI 1_4).

Generally, an efficient strategy for identifying fragments that interact with the target is to screen the library at a single concentration of each fragment and to follow up with a second round of analysis using a concentration series of the fragments to confirm that interactions are concentration dependant, reach steady-state within the injection time and do not interact super-stoichiometrically. A pseudo steady-state
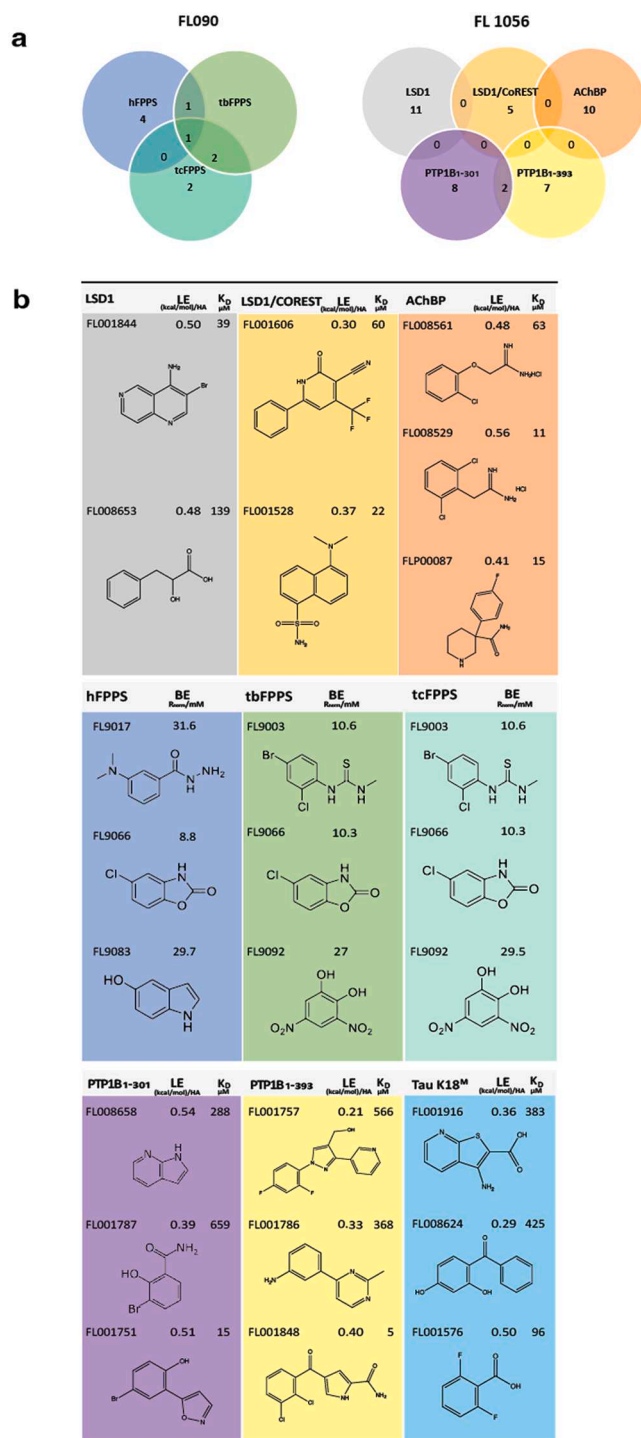
analysis (based on report points at the end of the injection irrespective if this represented steady-state or not) is useful as a means of establishing a concentration dependency, but not for quantification of affinities. An average of 10 % of hits from the initial screen are typically taken to the next step.

3.3. Identification of fragments interacting with large and dynamic targets – AChBP

For large and structurally dynamic targets, the challenge is to determine if fragments bind to single or multiple binding sites, single or multiple conformational states and if signals are affected by conformational changes induced by ligand binding. To illustrate how these complexities can be addressed, we here use AChBP, a proxy for the large

Fig. 3. Secondary screening data and hit confirmation. a-c, Examples of sensorgrams with square pulse typical for fragments, *i.e.* fast association and dissociation kinetics (Fig. 2e, green). d-i, examples of sensorgrams for fragments exhibiting non-ideal interactions (Fig. 2e, red, yellow, blue). j-l, signal *vs.* concentration curves for sensorgrams in a-c. Solid curves are based on R_{norm} data fitted by nonlinear regression analysis to a simple 1:1 interaction (insufficient for quantification due to $K_D >>$ screening concentration). The dashed lines in m-u represent dose response plots for FPPS with the tangent representing the slopes of the graphs at low ligand concentrations, from which BE was estimated. The shown sensorgrams represent the reference subtracted data used for fitting.

Fig. 4. Screening outcome a. Venn Diagram highlighting identified hits for FL1056 (left) and FL90 (right). b, Table with structures of hit examples, ligand efficiency (LE), binding efficiency (BE) and apparent equilibrium dissociation constant ($K_{\mathrm{D}}^{\mathrm{app}}$) of a selection of fragment hits.

class of therapeutically relevant human Cys-loop receptor class of LGICs.

In order to generate a stable, high-density surface, AChBP was immobilised in a two-step process. It was first captured via a His-tag, followed by covalent coupling using amine coupling via lysine residues on the surface of the protein [44]. This has several advantages. Firstly, the negatively charged protein can be captured on the surface at neutral pH and does not have to be exposed to a buffer with very low pH which may affect its structure. Secondly, capture of the protein via the five His-tags in the pentamer (one per subunit) potentially results in a single orientation of the complex on the surface. Thirdly, covalent coupling results in an irreversibly bound protein. Overall, this procedure allowed the protein to be immobilised at a higher concentration than when using amine coupling directly and a more stable surface than when only relying on the interaction between the His-tag and the NTA-ligand. Lobeline confirmed that the generated AChBP surface was functional (Fig. SI 2_1).

As a first step, the FL1056 library was pre-screened at the intended screening conditions to identify potentially problematic fragments (see above). It resulted in exclusion of 32 fragments. Subsequently, via a single concentration screen at 250 μM, >100 fragment hits could readily be identified in the FL1056 library (Fig. 2a, right). Fragments interacting without discernible secondary binding complexities and response levels above a threshold set to result in the selection of 10 % of the screened compounds were considered hits. Fragments showing secondary effects indicative of conformational changes or slow dissociation were not selected as hits in the data analysis, even when they gave high signals (examples shown in Fig. SI 2_5). Such fragments may be of interest, but required more elaborate validation and have been followed up elsewhere (FitzGerald et al., manuscript in preparation).

Selected hits were followed-up by injecting them in a concentration series to confirm that the signal was concentration dependant and to estimate affinities and kinetics if possible. Due to the very rapid kinetics, only steady state analysis of the data was possible. Representative sensorgrams and dose-response plots are shown in Fig. 3a-b, and j-k, respectively. Ten fragments were confirmed as hits (Table 1) and gave data from which K_{D} values in the micro molar range could reliably be determined. Structures, LE- and K_{D}-values of hits are exemplified in Fig. 4b. These hits have been confirmed via X-ray crystallography and will be published elsewhere (FitzGerald et al., manuscript in preparation) [45].

3.4. Identification of fragments interacting with targets in protein complexes – LSD1

For identification of ligands specific for either exposed or potentially blocked surfaces in targets that are part of transient or stable macromolecular complexes, a useful strategy is to multiplex the screen and use sensor surfaces with the target alone as well as in complex with binding partners. To demonstrate the principle, we have used LSD1, a large and structurally complex target with multiple binding partners and several functions. To better understand the characteristics of LSD1 and its druggability, we were interested in identifying ligands targeting the active site (harbouring the protein substrate binding site and the FAD cofactor site), as well as ligands binding to the LSD1/CoREST protein-protein interaction surface or potential allosteric sites.

The challenges in this project were not only related to the structural complexity of LSD1, but also lack of suitable tool compounds. Although we had access to a compound for monitoring immobilisation and functionality of LSD1 alone (BEA1, see Fig. SI 2_1), the compound does not interact with LSD1 in the presence of CoREST. No tool compound was available for verifying the structural integrity of the LSD1/CoREST complex. The size of the complex was also an issue, considering the low signals expected from fragment interactions. Initial hit calling was therefore done with assays using a high-density sensor surface while subsequent follow-up and verification used lower density surfaces. This permits the detection of weakly binding fragments (*e.g.* Fig. 3c), whilst also controlling for limited mass transport and steric hindrance artifacts. In some cases, the data from higher concentrations of fragments have to be omitted due to strong non-specific binding events, *i.e.* super-stoichiometric binding, as exemplified by the top sensorgrams in Fig. 3f and i. Hits were selected on the basis of sensorgram shape and affinity, estimated from dose-response plots using report points taken at steady state.

Using this set up, FL1056 was screened at 250 μM against LSD1 alone

and the LSD1/CoREST complex. It enabled the discrimination of hits specific for the planar surface of the tower domain of LSD1, and hits that are not sensitive to the binding of the cofactor and thus bind elsewhere. A similar number of hits were identified in the primary screen against LSD1 alone (107 compounds), compared to that against LSD1/CoREST (110 compounds), but a larger number could be confirmed for LSD1 alone (11 compounds) than the complex (5 compounds) (Table 1). This suggests that the interface between LSD1 and CoREST could be a hotspot for fragment binding. There was no overlap between the confirmed hits, indicating that they are not simply non-specific binders (Fig. 4a). The structures of some hits with micro molar K_D-values are exemplified in Fig. 4b, showing the types of fragments identified. (Orthogonal confirmation of hits is done elsewhere.)

3.5. Identification of fragments interacting with structurally variable or unstable targets – FPPS

Multiplexed approaches can also be useful for overcoming problems associated with unstable targets and for which the structural integrity of the target is unknown or varies. FPPS is known to be structurally dynamic, as for example demonstrated by X-ray crystallography experiments which failed to model several solvent exposed loop regions [25]. FPPS from three different species was used to demonstrate how to implement a multiplexed approach when also suitable tool compounds are unavailable.

The data generated for FPPS is based on screening a small fragment library (FL90) in three independent experiments. Initially, a single channel system was used to address the three FPPS variants and a reference surface with the same injection of analyte (two independent screens). The library was also screened using a multi-channel system where each species variant of FPPS was immobilized in a separate channel also containing a blank reference surface.

The rationale for overcoming the lack of reference compounds for checking target functionality was based on the fact that the enzyme is dependant on Mg^{2+} as a cofactor, structuring the active site in a catalytically competent state. It was consequently possible to generate two sets of data by screening the three enzymes in the absence and presence of the cofactor Mg^{2+}. By using the data from the experiment without the cofactor as a negative reference, it was possible to identify fragments selective for the structurally intact protein (Fig. 2b) [13]. The reliability of this approach was supported by the observation that a larger number of fragments interacted with surfaces in the absence of Mg^{2+}, indicative of non-specific binding to unfolded regions.

To illustrate how to identify compounds potentially binding to allosteric sites, we show the multiplexed data from the screening of FL90 against FPPS from three different species. Instead of relying on a reference surface with a blocked active site, the approach assumes that sites not directly involved in the catalytic reaction (here referred to as allosteric sites) are less well conserved between species and that potentially allosteric ligands can be identified amongst fragments that only interacted with one FPPS variant (i.e. not the conserved active site). This approach is suitable also for identifying species-selective ligands.

Although the fragments showed suboptimal interaction kinetic profiles with secondary effects (e.g. Fig. 3d and e), the same hits were identified irrespective of the instrument type, experimental design or immobilisation method, confirming the reliability of hit identification. The hit rate was ~15 %, with at least 10 hits identified and 3 confirmed for each target, with some overlap (Table 1 and Fig. 4a). Fragments previously identified to interact with tcFPPS were identified as hits also in these experiments [46]. Due to very low affinities, saturation of the binding was not seen with the highest concentrations in hit validation step using concentration series (Fig. 3m-u). It was therefore not possible to estimate K_D-values for the hits. Interactions were consequently quantified without a mechanistic/stoichiometric interpretation, via estimation of binding efficiencies (BE) from the interactions at low concentrations (explained in Fig. SI 1_4a). The structures of confirmed

fragment hits are exemplified in Fig. 4b.

3.6. Identification of fragments interacting with targets containing intrinsically disordered regions – PTP1B

Proteins containing intrinsically disordered regions (IDRs) represent a class of targets that may bind fragments to transiently exposed regions that lack a well-defined mode of interaction and specificity. It is a more extreme case of the problem illustrated for FPPS for which the overall structure appears to be relatively ordered, but where there is local disorder in a critical binding site. Here we illustrate how multiplexed screening can be performed against two variants of a target containing a large IDR, in this case PTP1B. The protein contains an IDR at its C-terminus. For the purpose of screening for ligands, we used two engineered forms of PTP1B: PTP1B$_{1-301}$ encompassing the folded catalytic phosphatase domain, and PTP1B$_{1-393}$ also encompassing the IDR. This enables the identification of two classes of hits, one potentially specific for the IDR included in PTP1B$_{1-393}$, and another for the folded domain common to PTP1B$_{1-301}$ and PTP1B$_{1-393}$.

Both PTP1B surfaces were confirmed to be functional using suramin (see Fig. SI 2_2). The interaction was the same with both constructs, indicating that suramin interacts with the folded, catalytic domain of PTP1B and that it is not affected by the presence of the IDR region of PTP1B$_{1-393}$ [47]. It was later used as a positive control at 7.5 μM in the screen, the highest concentration that could be used without signals being affected by non-specific interactions. FL1056 was screened against these two forms of PTB1B after a pre-screen removing potentially problematic fragments under the selected assay conditions. The hits for the two surfaces were compared (Fig. 2c). The screening data was normalized to account for differences in immobilization levels and functionality. To avoid potential remaining minor mismatches between the surfaces, the standard automatic hit prioritization workflow was complemented by a manual assessment of the hits. The importance of the manual assessment of selected hits is illustrated for a hit automatically selected for PTP1B$_{1-393}$, but not for PTP1B$_{1-301}$ (Fig. 2c, bottom, left, the arrow points to the fragment).

Using these procedures, a set of eight hits, unique for the folded domain (PTP1B$_{1-301}$), seven specific hits for the IDR (i.e. binding only to PTP1B$_{1-393}$) and two hits in common were identified (Table 1 and Fig. 4). However, none of the IDR-specific hits could be validated when re-analysed with the SPR biosensor assay. Still, analysis of the hits using differential scanning fluorimetry (DSF) confirmed several hits for both PTP1B$_{1-301}$ and PTP1B$_{1-393}$. The structures of some fragment hits and their estimated K_D and ligand efficiencies (LE) are presented in Fig. 4b. The challenge to confirm hits for PTP1B$_{1-393}$ is consistent with the elusive nature of intrinsically disordered targets and emphasizes the need for suitable orthogonal methods for confirming hits.

3.7. Identification of fragments interacting with aggregation-prone proteins – tau K18^M

Protein engineering and different surface designs can be used also to address problems associated with aggregation-prone targets. Here we used an engineered monomeric form of human tau K18 (tau K18^M) [28] as a model system [30]. Since the immobilisation of the protein on the sensor surface is a particularly critical step for aggregation-prone targets, it is advantageous to use sensor surfaces with different characteristics. This can be achieved by selecting different sensor chip types or using different immobilisation procedures. In addition, in order to avoid non-specific interactions with a highly charged protein such as tau K18^M, also the ionic strength and the pH of the buffer used in the screening are critical factors that should be optimised.

A two-step procedure was used to screen the FL1056 library. In the first step, it was screened against tau K18^M immobilized via amine coupling, a method resulting in a heterogenous surface with random orientation of the target. In a second step, identified hits were re-tested

against biotinylated Avi-tagged tau K18^M immobilized via streptavidin capture, thus limiting the heterogeneity of the protein surface. More than 100 hits were identified in the first step, with 45 subsequently confirmed in the second step and 19 selected for follow-up (Table 1). Sensorgrams for three hits interacting with both surfaces are shown in Fig SI 2_4. Structures and data for three hits are shown in Fig. 4b.

4. Discussion

SPR biosensors and methods for identifying fragment hits have developed significantly since our first report of using this technology for FBDD [11]. During this time, a number of alternative methods for screening and characterization of hits using SPR-based approaches have emerged. We have here illustrated the use of multiplexed methods involving multiple sensor surface combinations and experimental conditions for screening of fragment libraries and identifying hits using contemporary SPR biosensors, thereby expanding the range of targets and libraries that can be used. The panel of targets was selected to illustrate different experimental challenges and how multiplexed methods can be used to overcome them.

The focus has been to illustrate experimental designs suitable with respect to the features of the target, desired hits, availability of target variants and tool compounds. The study was limited to demonstrating how to use SPR-based methods to identify fragment hits and to confirm that they have appropriate interactions with the target. However, to ensure that the selection is not based on method artifacts it is essential to validate fragments using orthogonal methods. Such validation is not included here since such strategies need to be tailored specifically for each target.

The first aspect highlighted here is the importance of using libraries containing fragments with adequate solubility and features minimizing non-specific interactions with the protein or sensor surfaces under the conditions used for experiments. This is beyond the basic requirement that they should be structurally diverse and contain compounds possible to progress into leads. The commercial availability of small fragment libraries, for example designed for crystallography studies, provide a useful option for small screening campaigns when protein is scarce or unstable while still allowing chemical space to be adequately explored. The choice of library should consequently consider fragment solubility, sample format (powder or stock solution) and cost, seeing that higher concentration may be required for challenging targets and handling issues affect both consumption and experimental time.

Secondly, it is essential to use high-quality target protein that can be immobilised to sensor surfaces in a fully functional form and at a high density, thus generating functional sensor surfaces that are stable during the entire screen. This may require engineering of the protein, e.g. increasing its stability or introducing immobilisation tags. A reference compound with known interaction characteristics with the target should be available to control that target sensor surfaces interact with ligands in an expected manner and are functional during the entire experiment. Methods for confirming the functionality of the current sample before use and the suitability conditions used for preparation of sensor surfaces and screening are critical. Tool compounds may also be used for competition screening where potential fragment binding sites are blocked. In addition, isoforms and engineered variants with modifications in critical sites allows comparisons of interactions with different surfaces and indirectly identifying the location of binding sites for hits or their specificity for a certain isoform.

A third aspect highlighted here is the importance of dedicated experimental design, where the flexible features of advanced instruments are exploited. Recent technology developments enable higher throughput and faster screening campaigns, which benefits the screening of larger libraries. When multiplexing is not required and both target and fragments are readily available, the highest throughput can be achieved using systems with single sensor surfaces in parallel flow channels. A more elaborate experimental design, allowing the

identification of unique hits based on multiple selection criteria and lower material consumption, can be achieved using flow cells with several sensor surfaces but at the cost of lower throughput. For example, it is advantageous to use a combination of different surfaces when multiple target variants differing in sequence or length are available, while different injection protocols and competition experiments can be used when suitable tool compounds are available. Varying the experimental conditions (e.g. pH, ionic strength and temperature) is an option when the target protein allows this.

Finally, experiments need to be evaluated using appropriate data analysis procedures, tailored specifically for each project. There are numerous ways to pick hits, and the method should be selected with respect to several criteria, including the experimental repertoire for orthogonal confirmation available in the lab. The standard method is to select fragment hits with a signal above a certain threshold (typically relative a reference compound) at a certain time point and that has the typical square sensorgram shape. When reference compounds are not available, selection can instead be done by comparison to relevant reference surfaces, for example using target variants. Moreover, hits with non-square sensorgrams can be of interest, as it can show the ability of fragments to induce conformational changes, relevant for dynamic targets.

Overall, the two libraries and the panel of targets used here show that the outcome of a screen varies considerably and success cannot be predicted beforehand. For example, hit identification depends on the complexity of the data. Simple interaction profiles, i.e. rapid association and dissociation kinetics and expected binding stoichiometry, were typically observed in the FL1056 screens, and most commonly for AChBP. Suboptimal interaction profiles were common for hits from the FL90 screen against FPPS, most likely due to the features of the targets rather than the library. Steady state was not achieved for several hits, particularly for the IDRs. Super-stoichiometric interactions were observed in some cases, especially for LSD1.

For structurally dynamic targets, it is not only the location and structural features of the binding site that is an aspect to consider, but also inherent challenges relating to the dynamics as such since energy losses arising from conformational transitions in the binding site affect the possibility to identify very weak interactions [48]. Moreover, secondary effects resulting in distorted sensorgrams can be confounding when selecting hits. In the example with AChBP, such fragments were not selected for validation and orthogonal confirmation, for simplicity. But they have been selected and analysed in a separate study, and confirmed to induce conformational changes in the target (Fitzgerald et al., manuscript in preparation). The possibility of simultaneously detecting binding and ligand-induced conformational changes using SPR biosensor assays [17] enables the discrimination of fragments that simply bind to the target from those that also induce a conformational change.

A multiplexed strategy allowed screening against a target (LSD1) in the presence and absence of a protein binding partner (CoREST), with the aim of identifying fragments with a potential to be evolved into leads perturbing protein-protein interactions. Since fragments are unlikely to have high enough affinities to interfere significantly with a protein-protein interaction, hits need to be evolved into more potent competitors before functional effects can be detected. The current approach, shows that it is possible to identify fragments binding to a protein-protein interaction interface and guide optimisation without relying on functional or structure-based studies. This strategy can be complemented or substituted by experiments with either truncated or mutant versions of the protein binding partner for identifying a certain binding site.

The multiplexed strategy shown for identifying potentially allosteric fragments using different structural states of three species variants of the target (FPPS) circumvents the need for protein engineering to generate structurally stable targets and overcomes the requirement of active site binding tool compounds, otherwise enabling the screening against the

target with a blocked active site which can directly identify allosteric ligands.

The challenges of identifying ligands for dynamic target proteins is particularly difficult for proteins with IDRs, a class of drug targets that is not generally amenable to rational drug discovery methods. However, screening against an intrinsically disordered protein is achievable if it has partially folded regions or if target variants can be engineered and tested in parallel. Several fragment hits were thus identified for the folded domain of PTP1B, but none of the hits potentially interacting specifically with the IDR of PTP1B could be confirmed, consistent with the elusive nature of unstructured regions. The screening against tau K18^M resulted in a similar outcome, but also showed that there is a higher risk of detecting fragments interacting non-specifically with IDRs than with fully folded proteins (incidentally also seen with FPPS). Such effects can potentially be counteracted by optimising the conditions, *e.g.* using higher salt concentrations. However, it is difficult to optimise the experimental conditions for an IDP as it requires a good understanding of the structural and physico-chemical characteristics of the protein. It was shown also for tau K18^M that the immobilisation strategy can be critical.

Procedures immobilising the target to the surface via a single attachment point, *e.g.* using biotin-streptavidin or antibody capture, can be used to avoid immobilising the target in a non-functional or non-native conformation, as might be the case when using a multipoint attachment, such as amine coupling. Engineering of the target for optimal immobilisation may therefore be beneficial.

5. Conclusions

Novel instrumentation and improved understanding of how to implement SPR biosensors for FBLD broadens the range of targets that can be used for SPR biosensor-driven FBDD. Practical solutions to challenging targets are emerging and they do therefore not have to be seen as inherently problematic but simply require additional assay development. The identification of fragment hits needs to consider the weak signals, rapid kinetics and low affinities expected from fragments. The multiplexed approaches used here resulted in at least a handful of fragments interacting with each target, corresponding to a hit rate of 5–10 %. Still, target characteristics, the availability of tool compounds and reliable orthogonal assays for confirmation of hits influence the chance for success.

Author contributions

U.H.D. conceptualized and supervised the overall project. I.J.P.E., M. W., P.O.B., H.F.K., J.E.M.K. and D.J.H. provided synthetic compounds. E.A.F. collated and curated fragment library FL1056. H.F.K. performed fragment library analysis. E.A.F., V.O.T. and M.L.A. produced AChBP, LSD1 and LSD1/CoREST. E.A.F. designed and performed SPR experiments with AChBP, LSD1 and LSD1/CoREST. D.V. produced PTP1B and tau K18^M variants, and designed and performed SPR with PTP1B and tau K18^M variants. This work was supervised by B.D. and R.E.H. G.O. produced FPPS variants, and designed and performed SPR experiments with the FPPS variants. A.M., M.T.L. and C.H. supported the SPR biosensor experiments by providing access to instrumentation and technical expertise. E.A.F., D.V., and G.O. drafted the manuscript. E.A.F. and D.V. prepared figures. E.A.F. and U.H.D. finalized the manuscript.

Funding

Declaration of Competing Interest

Acknowledgments

Supplementary materials

Supplementary material associated with this article can be found, in the online version, at doi:10.1016/j.slasd.2023.09.001.

References

[1] Shuker SB, Hajduk PJ, Meadows RP, et al. Discovering high-affinity ligands for proteins: SAR by NMR. Science 1996;274:1531–4.

[2] Rees DC, Hirsch AKH, Erlanson DA. Introduction to the themed collection on fragment-based drug discovery. RSC Med Chem 2022;13:1439.

[3] Congreve M, Carr R, Murray C, et al. A 'rule of three' for fragment-based lead discovery? Drug Discov Today 2003;8:876–7.

[4] Jhoti H, Williams G, Rees DC, et al. The 'rule of three' for fragment-based drug discovery: where are we now? Nat Rev Drug Discov 2013;12:644–5.

[5] Tsai J, Lee JT, Wang W, et al. Discovery of a selective inhibitor of oncogenic B-Raf kinase with potent antimelanoma activity. Proc Natl Acad Sci U S A 2008;105: 3041–6.

[6] Murray CW, Newell DR, Angibaud P. A successful collaboration between academia, biotech and pharma led to discovery of erdafitinib, a selective FGFR inhibitor recently approved by the FDA. Medchemcomm 2019;10:1509–11.

[7] Walsh L, Erlanson DA, de Esch IJP, et al. Fragment-to-Lead Medicinal Chemistry Publications in 2021. J Med Chem 2023;66:1137–56.

[8] Tap WD, Wainberg ZA, Anthony SP, et al. Structure-Guided Blockade of CSF1R Kinase in Tenosynovial Giant-Cell Tumor. N Engl J Med 2015;373:428–37.

[9] Yeung DT, Shanmuganathan N, Hughes TP. Asciminib: a new therapeutic option in chronic-phase CML with treatment failure. Blood 2022;139:3474–9.

[10] Hong DS, Fakih MG, Strickler JH, et al. KRAS(G12C) Inhibition with Sotorasib in Advanced Solid Tumors. N Engl J Med 2020;383:1207–17.

[11] Nordstrom H, Gossas T, Hamalainen M, et al. Identification of MMP-12 inhibitors by using biosensor-based screening of a fragment library. J Med Chem 2008;51: 3449–59.

[12] Danielson UH. Fragment library screening and lead characterization using SPR biosensors. Curr Top Med Chem 2009;9:1725–35.

[13] Luttens A, Gullberg H, Abdurakhmanov E, et al. Ultralarge Virtual Screening Identifies SARS-CoV-2 Main Protease Inhibitors with Broad-Spectrum Activity against Coronaviruses. J Am Chem Soc 2022;144:2905–20.

[14] Sixma TK, Smit AB. Acetylcholine binding protein (AChBP): a secreted glial protein that provides a high-resolution model for the extracellular domain of pentameric ligand-gated ion channels. Annu Rev Biophys Biomol Struct 2003;32:311–34.

[15] Seeger C, Christopeit T, Fuchs K, et al. Histaminergic pharmacology of homo-oligomeric beta3 gamma-aminobutyric acid type A receptors characterized by surface plasmon resonance biosensor technology. Biochem Pharmacol 2012;84: 341–51.

[16] Spurny R, Debaveye S, Farinha A, et al. Molecular blueprint of allosteric binding sites in a homologue of the agonist-binding domain of the alpha7 nicotinic acetylcholine receptor. Proc Natl Acad Sci U S A 2015;112:E2543–52.

[17] Geitmann M, Retra K, de Kloe GE, et al. Interaction kinetic and structural dynamic analysis of ligand binding to acetylcholine-binding protein. Biochemistry 2010;49: 8143–54.

[18] Shi Y, Lan F, Matson C, et al. Histone demethylation mediated by the nuclear amine oxidase homolog LSD1. Cell 2004;119:941–53.

[19] Kim SA, Zhu J, Yennawar N, et al. Crystal Structure of the LSD1/CoREST Histone Demethylase Bound to Its Nucleosome Substrate. Mol Cell 2020;78:903–14. e4.

[20] Yang FF, Xu XL, Hu T, et al. Lysine-Specific Demethylase 1 Promises to Be a Novel Target in Cancer Drug Resistance: therapeutic Implications. J Med Chem 2023;66: 4275–93.

[21] Noce B, Di Bello E, Fioravanti R, et al. LSD1 inhibitors for cancer treatment: focus on multi-target agents and compounds in clinical trials. Front Pharmacol 2023;14: 1120911.

[22] Duschak VG. Major Kinds of Drug Targets in Chagas Disease or American Trypanosomiasis. Curr Drug Targets 2019;20:1203–16.

[23] Park J, Pandya VR, Ezekiel SJ, et al. Phosphonate and Bisphosphonate Inhibitors of Farnesyl Pyrophosphate Synthases: a Structure-Guided Perspective. Front Chem 2020;8:612728.

[24] Feng Y, Park J, Li SG, et al. Chirality-driven mode of binding of alpha-aminophosphonic acid-based allosteric inhibitors of the human farnesyl pyrophosphate synthase (hFPPS). J Med Chem 2019;62:9691–702.

[25] Munzker L, Petrick JK, Schleberger C, et al. Fragment-based discovery of non-bisphosphonate binders of Trypanosoma brucei Farnesyl Pyrophosphate Synthase. Chembiochem 2020;21:3096–111.

[26] Han S, Li X, Xia Y, et al. Farnesyl pyrophosphate synthase as a target for drug development: discovery of natural-product-derived inhibitors and their activity in pancreatic cancer cells. J Med Chem 2019;62:10867–96.

[27] Liu R, Mathieu C, Berthelet J, et al. Human protein tyrosine phosphatase 1B (PTP1B): from structure to clinical inhibitor perspectives. Int J Mol Sci 2022;23.

[28] Evans R, Ramisetty S, Kulkarni P, et al. Illuminating intrinsically disordered proteins with integrative structural biology. Biomolecules 2023:13.

[29] Hosoya Y, Ohkanda J. Intrinsically Disordered Proteins as Regulators of Transient Biological Processes and as Untapped Drug Targets. Molecules 2021:26.

[30] Yeboah F, Kim TE, Bill A, et al. Dynamic behaviors of alpha-synuclein and tau in the cellular context: new mechanistic insights and therapeutic opportunities in neurodegeneration. Neurobiol Dis 2019;132:104543.

[31] Biernat J, Gustke N, Drewes G, et al. Phosphorylation of Ser262 strongly reduces binding of tau to microtubules: distinction between PHF-like immunoreactivity and microtubule binding. Neuron 1993;11:153–63.

[32] Vagrys D, Davidson J, Chen I, et al. Exploring IDP-Ligand Interactions: tau K18 as A Test Case. Int J Mol Sci 2020;21.

[33] Arvidsson PI, Sandberg K, Forsberg-Nilsson K. Open for collaboration: an academic platform for drug discovery and development at SciLifeLab. Drug Discov Today 2016;21:1690–8.

[34] Huschmann FU, Linnik J, Sparta K, et al. Structures of endothiapepsin-fragment complexes from crystallographic fragment screening using a novel, diverse and affordable 96-compound fragment library. Acta Crystallogr F Struct Biol Commun 2016;72:346–55.

[35] Sauer WH, Schwarz MK. Molecular shape diversity of combinatorial libraries: a prerequisite for broad bioactivity. J Chem Inf Comput Sci 2003;43:987–1003.

[36] Celie PH, van Rossum-Fikkert SE, van Dijk WJ, et al. Nicotine and carbamylcholine binding to nicotinic acetylcholine receptors as studied in AChBP crystal structures. Neuron 2004;41:907–14.

[37] FitzGerald EA, Butko MT, Boronat P, et al. Discovery of fragments inducing conformational effects in dynamic proteins using a second-harmonic generation biosensor. RSC Adv 2021;11:7527–37.

[38] Yang J, Talibov VO, Peintner S, et al. Macrocyclic Peptides Uncover a Novel Binding Mode for Reversible Inhibitors of LSD1. ACS Omega 2020;5:3979–95.

[39] Opassi G, Nordstrom H, Lundin A, et al. Establishing Trypanosoma cruzi farnesyl pyrophosphate synthase as a viable target for biosensor driven fragment-based lead discovery. Protein Sci 2020;29:991–1003.

[40] Johnsson B, Lofas S, Lindquist G. Immobilization of proteins to a carboxymethyldextran-modified gold surface for biospecific interaction analysis in surface plasmon resonance sensors. Anal Biochem 1991;198:268–77.

[41] Elinder M, Geitmann M, Gossas T, et al. Experimental validation of a fragment library for lead discovery using SPR biosensor technology. J Biomol Screen 2011; 16:15–25.

[42] Genick CC, Barlier D, Monna D, et al. Applications of Biophysics in High-Throughput Screening Hit Validation. J Biomol Screen 2014;19:707–14.

[43] Gustafsson SS, Vrang L, Terelius Y, et al. Quantification of interactions between drug leads and serum proteins by use of "binding efficiency". Anal Biochem 2011; 409:163–75.

[44] Kimple AJ, Muller RE, Siderovski DP, et al. A capture coupling method for the covalent immobilization of hexahistidine tagged proteins for surface plasmon resonance. Methods Mol Biol 2010;627:91–100.

[45] Cederfelt D. Structural studies of drug targets and a drug metabolizing enzyme. PhD Thesis, Uppsala university 2023.

[46] Opassi G, Nordström H, Lundin A, et al. Establishing Trypanosoma cruzi farnesyl pyrophosphate synthase as a viable target for biosensor driven fragment-based lead discovery. Protein Science 2020;29:977–89.

[47] Zhang YL, Keng YF, Zhao Y, et al. Suramin is an active site-directed, reversible, and tight-binding inhibitor of protein-tyrosine phosphatases. J Biol Chem 1998;273: 12281–7.

[48] Brandt P, Geitmann M, Danielson UH. Deconstruction of non-nucleoside reverse transcriptase inhibitors of human immunodeficiency virus type 1 for exploration of the optimization landscape of fragments. J Med Chem 2011;54:709–18.